



# Solvent-induced assembly of mono- and divalent silica nanoparticles

Bin Liu, Etienne Duguet, Serge Ravaine

## ► To cite this version:

Bin Liu, Etienne Duguet, Serge Ravaine. Solvent-induced assembly of mono- and divalent silica nanoparticles. Beilstein Journal of Nanotechnology, 2023, 14, pp.52-60. 10.3762/bjnano.14.6 . hal-03932132

HAL Id: hal-03932132

<https://hal.science/hal-03932132>

Submitted on 10 Jan 2023

**HAL** is a multi-disciplinary open access archive for the deposit and dissemination of scientific research documents, whether they are published or not. The documents may come from teaching and research institutions in France or abroad, or from public or private research centers.

L'archive ouverte pluridisciplinaire **HAL**, est destinée au dépôt et à la diffusion de documents scientifiques de niveau recherche, publiés ou non, émanant des établissements d'enseignement et de recherche français ou étrangers, des laboratoires publics ou privés.

# **Solvent-induced assembly of mono- and divalent silica nanoparticles**

Bin Liu<sup>1,‡</sup>, Etienne Duguet<sup>2</sup>, Serge Ravaine<sup>\*1</sup>

<sup>1</sup>Univ. Bordeaux, CNRS, CRPP, UMR 5031, 33600 Pessac, France.

<sup>2</sup>Univ. Bordeaux, CNRS, Bordeaux INP, ICMCB, UMR 5026, 33600 Pessac, France

<sup>‡</sup>Present address : School of Chemistry and Chemical Engineering, Liaocheng University, Liaocheng 252059, P. R. China

Email: serge.ravaine@crpp.cnrs.fr

## **Abstract**

Particles with attractive patches are appealing candidates for use as building units in the objective of fabricating novel colloidal architectures by self-assembly. Here, we report the synthesis of one-patch silica nanoparticles, which consist of silica half-spheres of which the concave face carries in its center a polymeric patch made of grafted polystyrene chains. The multistage synthesis allows a fine control of the patch-to-particle size ratio from 0.23 to 0.57. The assembly of the patchy nanoparticles can be triggered by reducing the solvent quality for the polystyrene chains. Dimers or trimers can be obtained by tuning the patch-to-particle size ratio. When mixed with two-patch nanoparticles, the one-patch nanoparticles control the length of the resulting chains, by behaving as colloidal chain stoppers. The present strategy allows the future elaboration of novel colloidal structures by controlled assembly of nanoparticles.

## **Keywords**

Patchy nanoparticles; assembly; patch-to-particle size ratio; chain stopper

## **Introduction**

Colloidal engineering has become an enormous research effort, with a major focus placed on creating increasingly smart particles scalably, such that desired structures can be assembled in a bottom-up fashion [1-5]. Among all the existing synthetic routes permitting to imbue functionality into a colloidal suspension, those dedicated to the formation of patchy particles have received particular attention [6-10]. Indeed, several generic models including the extended Kern and Kern-inspired patchy models [11-13], the spot-like patchy models [14-15], and the rigid-body patchy models [16-17] have shown the great potentiality of patchy particles to serve as building blocks for the assembly of an exotic variety of colloidal structures. Experimentally, depletion interactions have been utilized to drive particles with a spherical cavity and complementary microspheres to form colloidal clusters [18]. Colloidal chains have been obtained by the assembly of Janus particles with one face selectively functionalized with DNA having self-complementary sticky end [19], particles with two patches functionalized with metal-coordination-based recognition units [20] and by co-assembly of block copolymer micelles and hard nanoparticles [21]. Particles with two patches located at the opposite poles have been assembled into a Kagome lattice by hydrophobic interactions [22], into chains by liquid bridging [23] and into a series of structures under AC electric field [24]. The linear self-assembly of patchy gold nanorods tethered with hydrophobic polymer chains at both ends has been triggered by solvophobic attractions induced by a change in solvent quality [25]. By using post-assembly ligand photo-cross-linking [26] or by adding monofunctional nanospheres

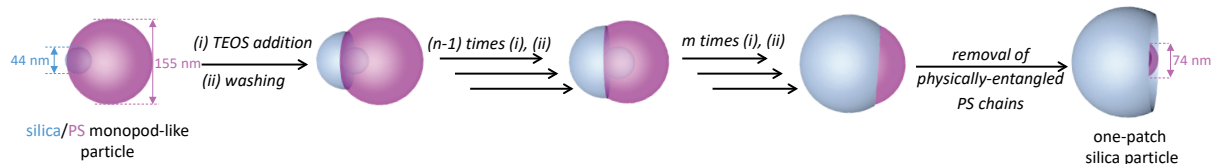
into a suspension of bifunctional gold nanorods [27], it was shown that the average degree of polymerization of the resulting chains could be controlled. The reduction of the solvent quality may be also employed to induce the assembly of silica/polystyrene dumbbells [28] and silica nanoparticles with two PS patches (2-PSN) [29-31] into multipod-like clusters and colloidal chains, respectively. We have recently reported that the same strategy can be used to assemble one-patch silica nanoparticles (1-PSN) with a well-controlled patch-to-particle size ratio (PPSR) into dimers, trimers, tetramers and spherical micelles at low incubation time in mixtures of tetrahydrofuran (THF) and ethanol [32]. Here, we extend the study to 1-PSN with smaller PPSR values and to the use of another poor solvent for the PS patch, *i.e.* salty water. We show that only dimers or trimers can be obtained, due to steric hindrance induced by the large silica cap of the patchy nanoparticles. The present study also extends the insights we gained recently about the capability of using 1-PSN with a PPSR of 0.60 as chain stoppers [31], as we show that the addition of 1-PSN with a lower PPSR value of 0.38 allows us to control the length of 2-PSN chains in a wider range of compositions.

## Results and Discussion

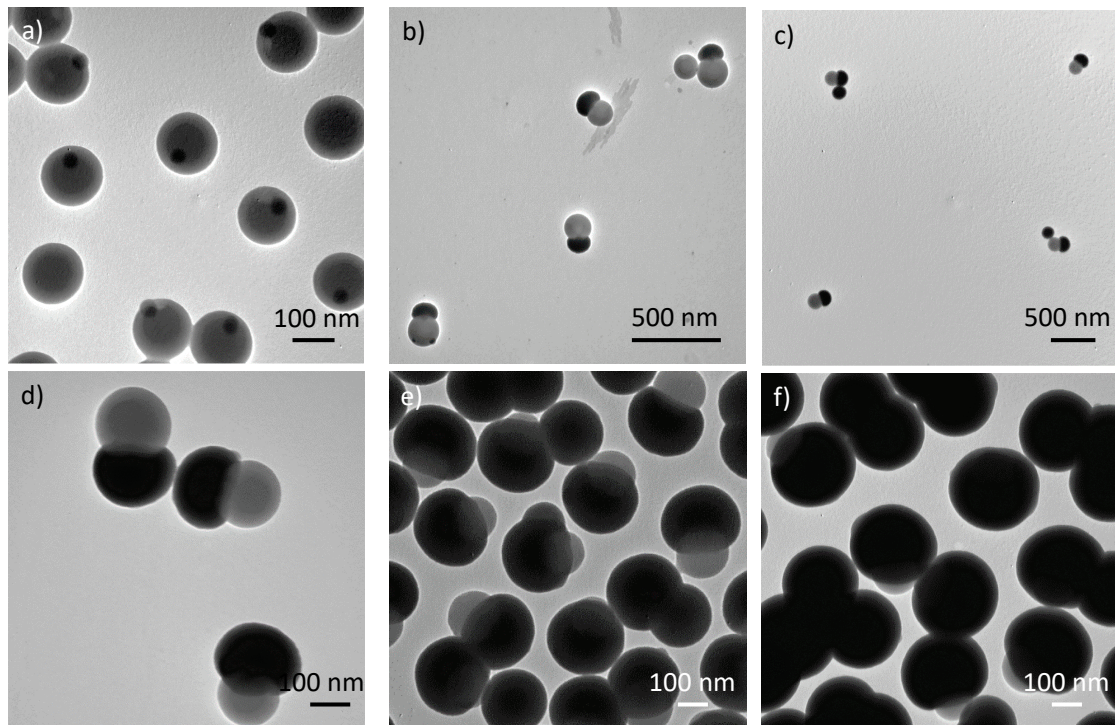
### Synthesis of one-patch silica particles with well-controlled patch-to-particle size ratio

Figure 1 shows the multi-step approach developed to synthesize 1-PSN with controlled patch size. First, silica/PS monopods consisting of a central silica core attached to one PS nodule (Figure 2 a) have been prepared by seeded-growth emulsion polymerization of styrene, as reported elsewhere [32] (see experimental details). The silica core of the silica/PS monopods was regrown through successive additions of a small amount of TEOS interspersed with centrifugation/redispersion cycles in order to avoid the

occurrence of secondary nucleation of silica [30]. Figures 2 b-f) show the morphology of the silica/PS nanoparticles after 1, 2, 4, 9 and 14 iterative silica growth steps, with measured diameter of the silica cap of 130, 165, 195, 250 and 315 nm, respectively. The selective dissolution of the physically-entangled PS chains by three centrifugation/redispersion cycles in 20 mL of THF was thus performed to get the 1-PSN with controlled PPSR, which is defined as the ratio of the diameter of the PS patch divided by the diameter of the silica cap.



**Figure 1:** Synthetic route for the preparation of 1-PSN with a controlled patch-to-particle size ratio.



**Figure 2:** TEM images of the silica/PS monopods after (a) 0, (b) 1, (c) 2, (d) 4, (e) 9, (f) 14 iterative silica growth steps.

As shown in Figure 3, it led to the formation of silica particles with one circular cavity, at the bottom of which the accessible surface of the initial silica seed is decorated by a PS shell of about 15 nm (as estimated by TEM). The latter is made up of covalently grafted PS macromolecules resulting from the copolymerization of styrene with the methacryloxyethyl groups. As demonstrated previously [25], these PS chains can serve as sticky patches when their solubility is reduced through the addition of a poor solvent. Therefore, the diameter of the patch is about 74 nm and the PPSR of the as-obtained 1-PSN varies from 0.23 to 0.57 (Figure 3).

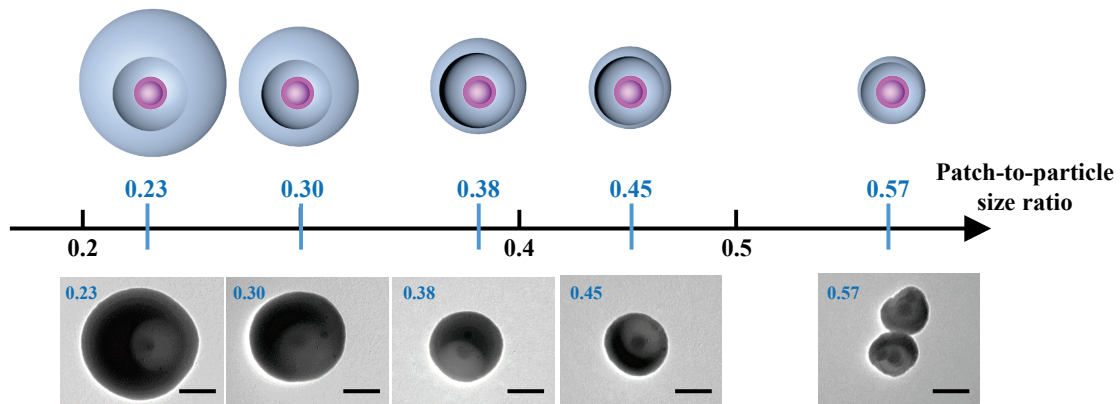


**Figure 3:** Schemes and representative TEM images of 1-PSN with PPSR varying from 0.23 to 0.57. Scale bars: 100 nm.

### Influence of the patch-to-particle size ratio on the self-assembly behaviour of one-patch silica particles

Our previous work on the assembly of 1-PSN with larger PPSR ranging from 0.69 to 1.54 in a THF/ethanol mixture has shown that colloids with a low aggregation number, e.g. dimers, trimers, tetramers and spherical micelles could be obtained at low

incubation time, and that the higher the PPSR value, the more these micelles evolved into larger objects over long incubation periods. They elongated in the form of chains for PPSR = 0.87 or extended into bilayers for PPSR = 1.18 or 1.54 [32]. Here, we first tried to assemble 1-PSN with PPSR ranging from 0.23 to 0.57 in THF/ethanol mixtures. Figure 4 a) shows all of them were found to be unable to self-assemble in the presence of ethanol, meaning that ethanol is not sufficient as bad solvent for PS to make the patches attractive enough and/or the macromolecular interactions strong enough to maintain the assembly. We performed other series of experiments by using pure water (Figure 4 b) or salty water (Figure 4 c) instead of ethanol in different fractions. We observed that, except for 1-PSN with  $\text{PPSR} \leq 0.3$ , assembly was possible and led to dimers and possibly to clusters of low aggregation number for the highest PPSR values. These results first indicate that the size of the silica cap of the 1-PSN has a strong influence on their capability to self-assemble. Indeed, when the regrown silica cap reaches a certain size, the PS chains which are grafted onto the initial silica seed surface and whose number-average mass was estimated to be  $\sim 500\ 000\ \text{g}\cdot\text{mol}^{-1}$  [33], can no longer interact because they are too far from each other. A closer examination of Figures 4 b-c) shows that water and even more so salty water is more efficient than ethanol to promote the assembly of 1-PSN. This is probably because salty water reduces both the electrostatic repulsions between nanoparticles due to negatively charged silanolate groups at their surface and the solvent quality for the PS macromolecules. Minimization of the free surface energy of the system thus corresponds to the formation of physical bonds between the latter [34,35], which thus behave as sticky patches. The kinetics of the assembly in a 7/3 (vol/vol) THF/salty water mixture was more deeply investigated. Figure 4 d) shows that the incubation of 1-PSN with a PPSR of 0.57 led to the formation of dimers, trimers and larger aggregates, whose number fraction after 10 days of incubation was 10%, 8% and 74%,

respectively. Interestingly, the incubation of 1-PSN with smaller and smaller PPSR progressively led to the formation of assemblies made of fewer and fewer 1-PSN (Figure 4 e-g)). More explicitly, only dimers and trimers were obtained from 1-PSN with a PPSR of 0.45, while only dimers were obtained when PPSR was 0.38.

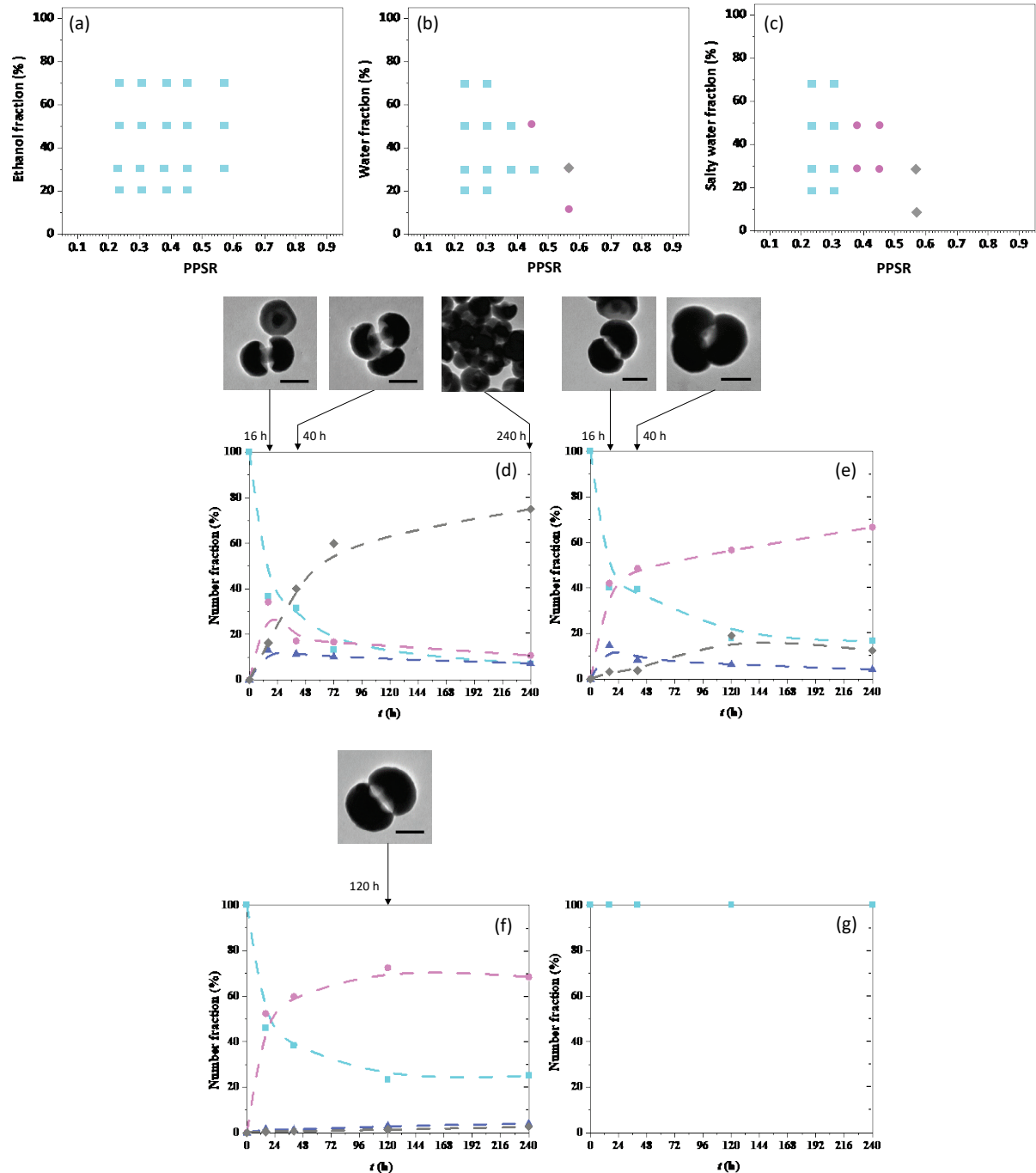


**Figure 4:** Phase diagrams identifying the main products of self-assembly (1-PSN (light blue squares), dimers (magenta circles) and large clusters (grey diamonds)), as a function of ethanol/water/salty water fraction and time of incubation. Microscopy images are shown above panels (d), (e), and (f), corresponding to the stages indicated by arrows: 16 h, 40 h, and 240 h.

function of the patch-to-particle size ratio of 1-PSN in different solvent mixtures after 10-days incubation at room temperature: a) THF/ethanol; b) THF/water and c) THF/salty water ( $[NaCl] = 20$  mmol/L). Evolution with incubation time in a 7/3 (vol/vol) THF/salty water mixture of the fractions of 1-PSN (light blue squares), dimers (magenta circles), trimers (blue triangles) and large clusters (grey diamonds), as determined by statistical analysis of the TEM images for different PPSR values: d) 0.57; e) 0.45; f) 0.38; g) 0.30 or 0.23. Dotted lines are a guide to the eye. Representative TEM images of dimers, trimers and large aggregates formed after 16 h, 40 h, 120 h or 240 h are shown on the top. Scale bars: 100 nm.

The stickiness of the PS chains in the presence of salty water was further exploited by mixing 1-PSN of two different PPSR. The aim here was not to get heterodimers, *i.e.* resulting from the assembly of two different 1-PSN, with a high yield since homodimers could also be formed, but to perform a proof-of-principle experiment to demonstrate that such complex structures could be obtained. Figure 5 a) shows that heterodimers were effectively obtained by mixing 1-PSN with a PPSR of 0.45 and 0.38. After 24 hours, the incubation medium consists of 1-PSN (~26%), heterodimers (~30.5%), homodimers made of two 1-PSN with a PPSR of 0.45 (~17.5%), homodimers made of two 1-PSN with a PPSR of 0.38 (~23%), and also heterotrimers (~1.5%), and homotrimers (~1.5%) (Figure 5 b).

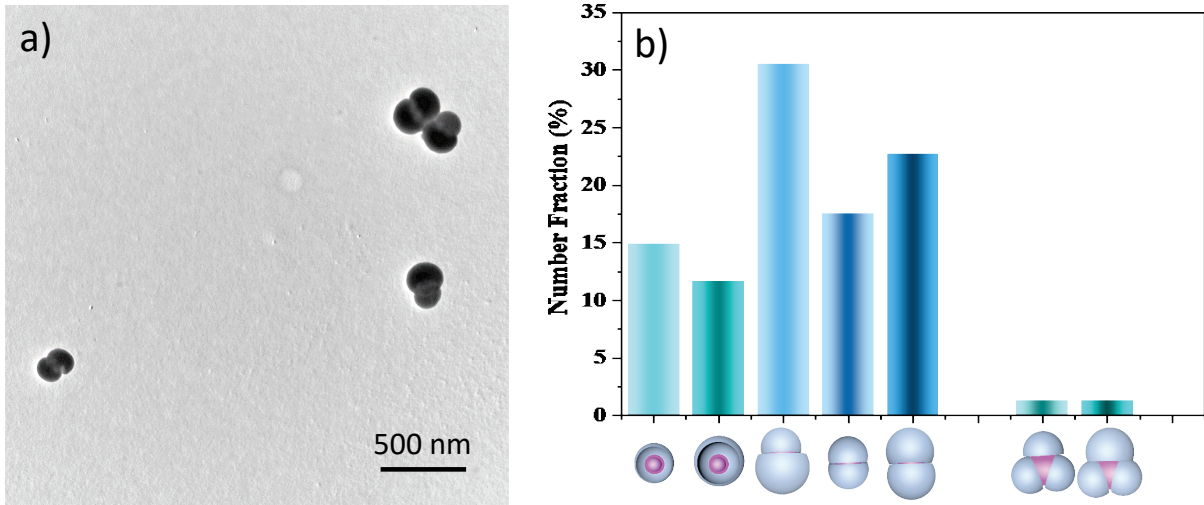


**Figure 5.** a) TEM image showing some heterodimers obtained after incubation in a 7/3 (vol/vol) THF/salty water mixture during 24 hours of a 1/1 mixture of 1-PSN with a PPSR of 0.45 and 0.38. b) Number distribution of 1-PSN of both sizes, homo- and heterodimers, homo- and heterotrimers present in the incubation medium after 24 hours, as determined by statistical analysis of TEM images.

### Co-assembly of 2-PSN and 1-PSN acting as chain-stoppers

It was previously shown that monofunctional nanoparticles can act as chain stoppers, as their addition into suspensions of soft patchy nano-particles [36], gold nanorods [27] or silver nanoplates [37] allowed the control of chain length. We thus studied the capability of the 1-PSN to act as chain stoppers when they are mixed with 2-PSN, whose solvent-induced assembly into colloidal polymers was recently reported [29-30]. Indeed, we previously showed that 2-PSN, which exhibit a disk-like morphology with a diameter of 190 nm, formed chains as long as 6  $\mu\text{m}$  (Figure 6 a, bottom row) when 30 vol % of salty water was added into the NP dispersion in THF, thereby reducing both the electrostatic repulsions between NPs due to negatively charged silanolate groups at their surface and the solvent quality for the PS chains [29]. The statistical analysis of the TEM images recorded from samples collected at different incubation times

allowed us to plot the time evolution of the number-average degree of polymerization,  $\bar{X}_n$ , defined as:

$$\bar{X}_n = \frac{\sum n_x x}{\sum n_x},$$

where  $x$  is the number of 2-PSN in the chain and  $n_x$  is the number of chains containing  $x$  2-PSN (Figure 6 b), magenta curve). The linear relationship which can be observed at short incubation time ( $t < 2$  h) is characteristic of a reaction-controlled step-growth polymerization, in which the reactivity of the patches is independent of the chain length [38]. At longer times ( $t > 2$  h), one can observe that  $\bar{X}_n$  does not vary linearly with time anymore (Figure 6 b). The polymerization of 2-PSN seems to follow a different pathway, that is, most likely, a “diffusion-controlled” stage, which can be possibly attributed to the fact that the sedimentation of the chains becomes the rate-limiting factor when they become relatively long. We recently reported that the length of the chains made of 105 nm or 130 nm 2-PSN can be controlled by the addition of 1-PSN with a PPSR of 0.60, which act as colloidal analogues of chain stoppers, at several [1-PSN]/[2-PSN] ratios between 0 and 0.5 [31]. Here we decide to further explore this behaviour by expanding the range of [1-PSN]/[2-PSN] ratios from 0 to 1.5. We thus first tried to co-assemble 190-nm 2-PSN with 1-PSN with a PPSR of 0.60. Figure 6 c) shows that even if a small proportion of chains are capped with 1-PSN, most of these ones are interspersed between the 2-PSN within the chains (red arrows), probably because of their small size. Assuming that the PPSR of 1-PSN should be at least equal to that of the 2-PSN so that they can play the role of chain stoppers, we thus decided to work with 1-PSN with a smaller PPSR of 0.38. Figure 6 a) shows that this time the 1-PSN are effectively located at both ends of the 2-PSN chains. In agreement with our previous results [31] and those reported by others [27, 37], Figure 6 a) shows that the chain length depends strongly of the 1-PSN/2-PSN ratio, as the higher it is, the shorter the chains after 120 hours of incubation. The chain stopper strategy allowed us to finely

tune the degree of polymerization at any incubation time, as shown in Figure 6 b). For instance, at  $t = 9$  h, the average number of 2-PSN in the chains is 10.7 in the absence of 1-PSN, whereas it is only equal to 3.2, 2.5 and 1.9 when the ratio 1-PSN/2-PSN is 0.5, 1 and 1.5, respectively.

## Conclusion

Following a multi-step approach based on the conformational enlargement of the silica core of silica/PS monopods that we recently developed [30-32], one-patch silica nanoparticles with a controlled patch-to-particle size ratio ranging from 0.23 to 0.57 were synthesized. The decrease of the solvent quality for the PS patch induced by the addition of salty water made it sticky, which induced the assembly of the patchy silica nanoparticles into mostly dimers when the interactions between the PS chains were not annihilated by steric hindrance between the silica parts. We also show that these one-patch silica nanoparticles can act as colloidal chain stoppers when they are mixed with divalent nanoparticles. We expect these results will inspire the fabrication of yet inaccessible colloidal structures by self-assembly. Bridging functionality at the colloidal chain end being now conceivable, their assembly into block-copolymer analogues can for instance be considered.

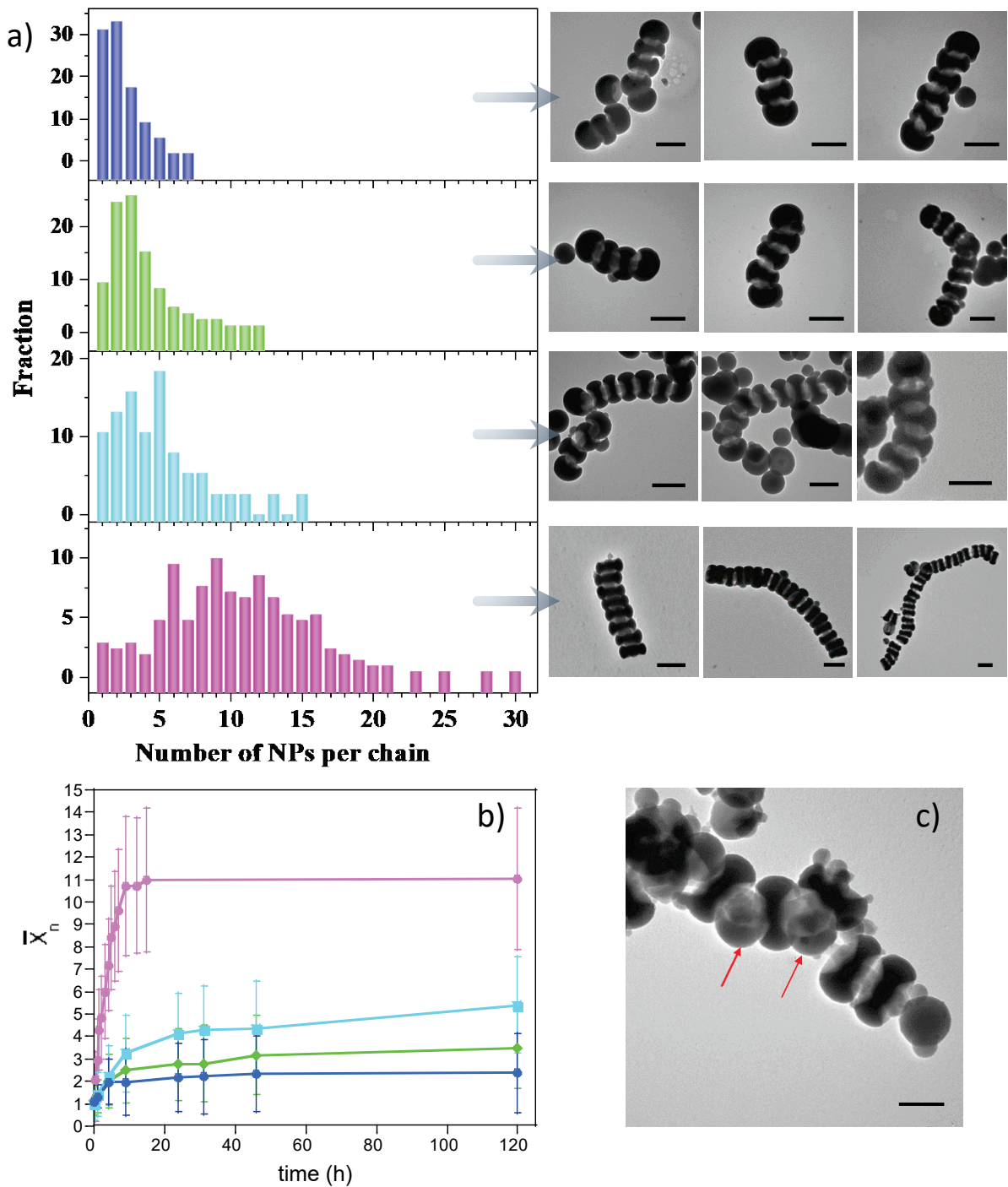


**Figure 6:** a) Chain length distribution and representative TEM images of chains for 1-PSN/2-PSN = 0 (magenta), 0.5 (light blue), 1 (green) and 1.5 (blue) at  $t = 120$  h. Scale bars: 200 nm. Experimental conditions are displayed in Table 1. b) Time dependence of  $\bar{X}_n$  for 1-PSN/2-PSN = 0 (magenta), 0.5 (light blue), 1 (green) and 1.5 (blue). Curves

are a guide to the eye. c) TEM image of a chain obtained by mixing 2-PSN with 1-PSN with a PPSR of 0.60 (1-PSN/2-PSN = 0.5; incubation time = 16 h). Scale bar: 100 nm.

## Experimental details

### Materials

We used styrene (Sigma-Aldrich, 99%), methacryloxymethyltriethoxysilane (MMS, ABCR, 98%), sodium persulfate (Sigma-Aldrich, 99%), Symperonic® NP30 (Aldrich), sodium dodecylsulfate (SDS, Sigma-Aldrich, > 90%), tetraethoxysilane (TEOS, Sigma-Aldrich, 99%), L-arginine (98.5 %, Sigma-Aldrich), ammonium hydroxide (28–30% in water, SDS), sodium chloride, ( $\geq$ 99.0%, Sigma-Aldrich), sodium hydroxide ( $\geq$ 98%, pellets, Sigma-Aldrich) as received. We systematically used ultrapure water with a resistivity of 18.2 MΩ•cm at 25°C obtained from a Milli-Q system (Millipore). We purchased absolute ethanol and tetrahydrofuran (THF, >99%) from VWR Chemicals.

### Synthesis of the silica/PS monopods and bipods

In a manner similar to the already reported procedure [32], monopods consisting of a central silica core attached to one PS nodule have been prepared by seeded-growth emulsion polymerization of styrene. Briefly, silica nanoparticles with an average diameter of  $44\pm2$  nm were obtained by TEOS hydrolysis/polycondensation according to a two-stage protocol. At the end of the synthesis, the silica surface was functionalized with methacryloxymethyl functions by reacting with MMS at room temperature for 3 hours and then one more hour at 90°C under stirring. The added MMS amount corresponded to a nominal grafting surface density of 0.7 funct./nm<sup>2</sup>. Then, the MMS-functionalized silica NPs ( $1.8\times10^{16}$  part/L) were used as seeds for the seed-growth emulsion polymerization of styrene (100 g/L) stabilized by a mixture (3 g/L) of Symperonic® NP30 and SDS (5 wt.%) and initiated by 1.3 mL Na<sub>2</sub>S<sub>2</sub>O<sub>8</sub> (0.1 g

dissolved in 4 mL water) at 70 °C for 6 h to obtain silica/PS monopods with a PS pod diameter of about 155 nm. The morphological yield was 99%.

Bipods consisting of a central silica core surrounded by two PS nodules with a diameter of about 160 nm were obtained with a yield of 97 % in a similar way from 55±2 nm silica nanoparticles which were functionalized with MMS at 0.5 funct./nm<sup>2</sup>.

### **Controlled growth of the silica core**

According to the procedure reported in [30], 9.1 mL of absolute ethanol, 0.7 mL of ammonia and 0.2 mL of the dispersion of monopods ( $1.8 \times 10^{16}$  part/L) or bipods ( $1.8 \times 10^{16}$  part/L) were introduced into a 25 mL flask and the mixture was homogenized using a magnetic bar. 200 µL of TEOS were added all at once after 5 min. The reaction was left under stirring at 20 °C for 15 min. The reaction medium was poured into a 50 mL Falcon tube containing 15 mL of absolute ethanol. After 2 cycles of centrifugation (12,000 g / 5 min) and redispersion in absolute ethanol, the nanoparticles were finally redispersed in 10 mL of a previously prepared hydroalcoholic solution (absolute ethanol/ammonia/water volume ratio: 91%/7%/2%). This protocol was renewed to obtain the next generation. The final diameter of the silica core of the bipods is 190 nm.

### **Dissolution of the PS nodules**

For dissolving the PS nodules of the monopods and bipods, three centrifugation/redispersion cycles in 20 mL of THF (12,000 g; 10 min) were performed. The concentration of 1-PSN and 2-PSN dispersions was adjusted to  $1.08 \cdot 10^{15}$  part/L and the solution was stored at 4 °C.

### **Assembly of one-patch silica nanoparticles**

Incubation of the nanoparticles was carried out in 15 mL tubes under rolling motion at 60 rpm at room temperature. A calculated volume of ethanol, water or salty water (20

mM NaCl aqueous solution) was added drop-by-drop under stirring into the THF dispersion of 1-PSN to reach the targeted volume fraction and a total volume of 1 mL. It took about 20 seconds for adding 100 µL. Assembled structures were monitored by collecting 50 µL samples at various incubation times and direct deposition on TEM grids.

### **Co-assembly of one- and two-patch silica nanoparticles**

Incubation of the nanoparticles in a 7/3 (vol/vol) THF/salty water mixture was carried out in 15 mL tubes under rolling motion at 60 rpm at room temperature. The composition of the mixtures is given in Table 1.

**Table 1.** Experimental conditions used for the co-assembly of 2-PSN and 1-PSN.

1-PSN/2-PSN particle ratio	volume (µL)			
	1-PSN dispersion	2-PSN dispersion	THF	salty water
0	0	700	1400	900
0.5	350	700	1050	900
1	700	700	700	900
1.5	1050	700	350	900

### **Characterization methods**

Transmission electron microscopy (TEM) experiments were performed using a Hitachi H600 microscope operating at an acceleration voltage of 75 kV. We prepared the samples by depositing one drop of the colloidal dispersion on conventional carbon-coated copper grids. We let the liquid evaporate in the open air at room temperature and placed the grids in a box away from dust. Statistics from image analysis were

performed over at least 300 multipods or 200 chains. The  $\zeta$  potential value of 1-PSN aqueous dispersions (pH ~5.7) was measured using the Malvern Zetasizer 3000 HS setup (Malvern Instruments). The dielectric constant of water was set to 80.4 and the Smoluchowsky constant  $f(ka)$  was 1.5.

## Funding

B. Liu was supported by a grant from the China Scholarship Council.

## References

- 1 S. C. Glotzer, M. Solomon and N. A. Kotov, Self-assembly: From nanoscale to microscale colloids, *AIChE J.*, 2004, 50, 2978–2985.
- 2 P. F. Damasceno, M. Engel and S. C. Glotzer, Predictive self-assembly of polyhedra into complex structures, *Science*, 2012, 337, 453–457.
- 3 A. P. Hynninen, J. H. Thijssen, E. C. Vermolen, M. Dijkstra and A. Van Blaaderen, Self-assembly route for photonic crystals with a bandgap in the visible region, *Nat. Mater.*, 2007, 6, 202–205.
- 4 L. Cademartiri, K. J. Bishop, P. W. Snyder and G. A. Ozin, Using shape for self-assembly, *Philos. Trans. R. Soc. A*, 2012, 370, 2824–2847.
- 5 J. D. Halverson and A. V. Tkachenko, DNA-programmed mesoscopic architecture, *Phys. Rev. E*, 2013, 87, 062310.
- 6 S. Ravaine and E. Duguet, Synthesis and assembly of patchy particles: Recent progress and future prospects, *Current Opinion in Colloid & Interface Science*, 2017, 30, 45–53.
- 7 G. R. Yi, D. J. Pine and S. Sacanna, Recent progress on patchy colloids and their self-assembly, *J Phys Condens Matter*, 2013, 25, 193101.

- 8 J. Du and R. K. O'Reilly, Anisotropic particles with patchy, multicompartiment and Janus architectures: preparation and application, *Chem Soc Rev.*, 2011, 40, 2402–2416.
- 9 A. B. Pawar and I. Kretzschmar, Fabrication, assembly, and application of patchy particles, *Macromol Rapid Commun.*, 2010, 31, 150–168.
- 10 E. Duguet, C. Hubert, C. Chomette, A. Perro and S. Ravaine, Patchy colloidal particles for programmed self-assembly, *Comptes Rendus Chim.*, 2016, 19, 173–182.
- 11 F. Sciortino, A. Giacometti and G. Pastore, Phase diagram of Janus particles, *Phys. Rev. Lett.*, 2009, 103, 237801.
- 12 A. Giacometti, F. Lado, J. Largo, G. Pastore and F. Sciortino, Phase diagram and structural properties of a simple model for one-patch particles, *J. Chem. Phys.*, 2009, 131, 174114.
- 13 F. Sciortino, A. Giacometti and G. Pastore, A numerical study of one-patch colloidal particles: from square-well to Janus, *Phys. Chem. Chem. Phys.*, 2010, 12, 11869–11877.
- 14 Z. Zhang, A. S. Keys, T. Chen and S. C. Glotzer, Self-assembly of patchy particles into diamond structures through molecular mimicry, *Langmuir*, 2005, 21, 11547–11551.
- 15 E. Bianchi, J. Largo, P. Tartaglia, E. Zaccarelli and F. Sciortino, Phase diagram of patchy colloids: towards empty liquids, *Phys. Rev. Lett.*, 2006, 97, 168301.
- 16 L. T. Yan, N. Popp, S. K. Ghosh and A. Boker, Self-assembly of Janus nanoparticles in diblock copolymers, *ACS Nano*, 2010, 4, 913–920.
- 17 T. D. Nguyen, C. L. Phillips, J. A. Anderson and S. C. Glotzer, Rigid body constraints realized in massively-parallel molecular dynamics on graphics processing units, *Comput. Phys. Commun.*, 2011, 182, 2307–2313.

- 18 S. Sacanna, W. T. M. Irvine, P. M. Chaikin and D. J. Pine, Lock and key colloids, *Nature*, 2010, 464, 575–578.
- 19 J. S. Oh, S. Lee, S. C. Glotzer, G. R. Yi and D. J. Pine, Colloidal fibers and rings by cooperative assembly, *Nat. Commun.*, 2019, 10, 3936.
- 20 Y. Wang, A. D. Hollingsworth, S. K. Yang, S. Patel, D. J. Pine and M. Weck, Patchy particle self-assembly via metal coordination, *J Am Chem Soc*, 2013, 135, 14064–14067.
- 21 Y. Cui, H. Zhu, J. Cai and H. Qiu, Self-regulated co-assembly of soft and hard nanoparticles, *Nat. Commun.*, 2021, 12, 5682.
- 22 Q. Chen, S. C. Bae and S. Granick, Directed self-assembly of a colloidal kagome lattice, *Nature*, 2011, 469, 381–384.
- 23 D. Lyu, W. Xu and Y. Wang, Low-symmetry MOF-based patchy colloids and their precise linking via site-selective liquid bridging to form supra-colloidal and supra-framework architectures, *Angew. Chem. Int. Ed.*, 2022, 61, e202115076.
- 24 Z. Wang, Z. Wang, J. Li and Y. Wang, Directional and reconfigurable assembly of metallocodielectric patchy particles, *ACS Nano*, 2021, 15, 5439–5448.
- 25 D. Fava, Z. Nie, M. A. Winnik and E. Kumacheva, Evolution of self-assembled structures of polymer-terminated gold nanorods in selective solvents, *Adv. Mater.*, 2008, 20, 4318–4322.
- 26 A. Lukach, K. Liu, H. Therien-Aubin and E. Kumacheva, Controlling the degree of polymerization, bond lengths, and bond angles of plasmonic polymers, *J Am Chem Soc.*, 2012, 134, 18853–18859.
- 27 A. Klinkova, H. Therien-Aubin, R. M. Choueiri, M. Rubinstein and E. Kumacheva, Colloidal analogs of molecular chain stoppers, *Proc. Natl. Acad. Sci.*, 2013, 110, 18775–18779.

- 28 W. Li, S. Ravaine and E. Duguet, Clustering of asymmetric dumbbell-shaped silica/polystyrene nanoparticles by solvent-induced self-assembly, *J. Colloid Interface Sci.*, 2020, 560, 639–648.
- 29 W. Li, B. Liu, C. Hubert, A. Perro, E. Duguet and S. Ravaine, Self-assembly of colloidal polymers from two-patch silica nanoparticles, *Nano Res.*, 2020, 13, 3371–3376.
- 30 B. Liu, S. Exiga, E. Duguet and S. Ravaine, Templated synthesis and assembly of two-, three- and six-patch silica nanoparticles with a controlled patch-to-particle size ratio, *Molecules*, 2021, 26, 4736.
- 31 B. Liu, W. Li, E. Duguet and S. Ravaine, Linear assembly of two-patch silica nanoparticles and control of chain length by coassembly with colloidal chain stoppers, *ACS Macro Letters* 2022, 11, 156-160.
- 32 B. Liu, S. Ravaine and E. Duguet, Solvent-induced assembly of one-patch silica nanoparticles into robust clusters, wormlike chains and bilayers, *Nanomaterials*, 2022, 12, 100.
- 33 C. Hubert, C. Chomette, A. Désert, M. Sun, M. Tréguer-Delapierre, S. Mornet, A. Perro, E. Duguet and S. Ravaine, Synthesis of multivalent silica nanoparticles combining both enthalpic and entropic patchiness, *Faraday Discuss.*, 2015, 181, 139–146.
- 34 K. Liu, Z. Nie, N. Zhao, W. Li, M. Rubinstein and E. Kumacheva, Step-growth polymerization of inorganic nanoparticles, *Science*, 2010, 329, 197–200.
- 35 R. M. Choueiri, E. Galati, A. Klinkova, H. Thérien-Aubin and E. Kumacheva, Linear assembly of patchy and non-patchy nanoparticles, *Faraday Discuss.*, 2016, 191, 198–204.

- 36 A. Gröschel, A. Walther, T. I. Löbling, F. H. Schacher, H. Schmalz and A. H .E. Müller, Guided hierarchical co-assembly of soft patchy nanoparticles, *Nature*, 2013, 503, 247–251.
- 37 B. Luo, J. W. Smith, Z. Wu, J. Kim, Z. Ou and Q. Chen, Polymerization-like co-assembly of silver nanoplates and patchy spheres, *ACS Nano*, 2017, 11, 7626–7633.
- 38 C. Yi, Y. Yang and Z. Nie, Alternating copolymerization of inorganic nanoparticles, *J. Am. Chem. Soc.*, 2019, 141, 7917–7925.